Squeezing-enhanced fiber Mach-Zehnder interferometer for low-frequency phase measurement

Fang Liu,[1] Yaoyao Zhou,[2] Juan Yu,[2] Jiale Guo,[1] Yang Wu,[1] Shixiong Xiao,[1] Dan Wei,[1] Yong Zhang,[1,a)] Xiaojun Jia,[2,b)] and Min Xiao[1,3]
[1]*National Laboratory of Solid State Microstructures, College of Engineering and Applied Sciences and School of Physics, Nanjing University, Nanjing 210093, China*
[2]*State Key Laboratory of Quantum Optics and Quantum Optics Devices, Institute of Opto-Electronics, Shanxi University, Taiyuan, Shanxi 030006, China*
[3]*Department of Physics, University of Arkansas, Fayetteville, Arkansas 72701, USA*

(Received 23 June 2016; accepted 23 December 2016; published online 9 January 2017)

We propose and experimentally demonstrate a quantum-enhanced fiber Mach-Zehnder interferometer for low-frequency phase measurement beyond the shot-noise limit using a high-frequency squeezing technique. The local oscillator field is amplitude-modulated in the MHz range and is then demodulated to avoid the technical noise that occurs at low frequencies. After measurement of the phase noise at a frequency of tens of kHz, an improvement of ~2 dB relative to the shot-noise level is achieved. Additionally, the amplitude modulation depth has no significant effect on the phase noise improvement of the interferometer when deployed in our experimental configuration. The current scheme introduces a quantum technique into the fiber-based measurements, particularly for the low frequency range, and this scheme has potential applications in the high-precision fiber sensing of temperature, strain, and various other parameters. *Published by AIP Publishing.*
[http://dx.doi.org/10.1063/1.4973895]

Precision phase measurement is an important metrology task. Various optical interferometers have been used to perform these measurements because of their high sensitivities.[1–6] To date, the most sensitive detectors of this type are the long-baseline laser interferometers that were designed for gravitational-wave detection. Their sensitivity can reach $\sim 10^{-23}\ \varepsilon\ \mathrm{Hz}^{-1/2}$ over the range from 100 Hz to 300 Hz,[7] where ε is the fractional length change. In recent years, optical fiber interferometers have attracted increasing attentions. Because of their unique advantages, including compact size, ease of deployment, high sensitivity, large bandwidth, and low cost,[8,9] fiber interferometers have been widely deployed for sensing of strain, sound, and acceleration in various environments, such as in oceans and on board aircraft.[10–13]

When a fiber or free-space interferometer is used to perform optical measurements, the sensitivity is ultimately limited by standard quantum noise, i.e., the shot-noise limit (SNL). In 1981, Caves theoretically showed that the squeezed state of light can be used to enhance interferometer sensitivity beyond the SNL.[14] Several subsequent experiments have demonstrated such quantum-enhanced interferometers.[15–18] In most of these experiments, the measured signal frequencies are above 1 MHz because it is relatively simple to achieve a squeezed state in this frequency range by avoiding the noise that occurs at low frequencies in these systems.[19–22] However, in many practical applications, such as position and strain sensing, the parameters to be measured tend to vary at much lower frequencies (typically in the kHz band). The types of technical noise in the low-frequency band, such as electric noise, seismic noise, and thermal noise, have prevented the application of these quantum-enhanced interferometers for decades. Major efforts have been made to develop low-frequency squeezed light sources.[23–28] Recently, several important technical issues in the development of low-frequency squeezing sources have been resolved. In 2006, Vahlbruch *et al.* demonstrated a coherent control scheme for stable phase-locking of the squeezed vacuum fields from 10 Hz to 10 kHz.[25] In 2012, Stefszky *et al.* presented a quantum-noise-limited balanced homodyne detection method with a flat shot-noise level down to 0.5 Hz.[29] When using such low-frequency squeezing sources, the noises in the audio-band frequencies must be handled carefully. The other approach is to use the high-frequency sidebands of the squeezed light for the low-frequency phase measurements. A high-frequency squeezed light source can operate in a MHz frequency regime where the classical noise sources have minimal impacts. Several theoretical schemes have been proposed to resolve the problems with this scheme using phase modulation techniques or a two-frequency interferometer.[30–33] However, experimental demonstrations are still required. In this Letter, we report the experimental demonstration of a quantum-enhanced fiber Mach-Zehnder interferometer (MZI) for phase measurements in the kHz band using a high-frequency (MHz range) squeezed state. In our experiments, the local light is amplitude-modulated (AM) at MHz frequencies. The interference signal is measured by the balanced heterodyne detection. Using this experimental configuration, the electronic and optical noises around the MHz modulation frequency enter the measurements rather than low-frequency noise. This method can thus technically avoid the low-frequency noise and allow the use of squeezed light in the MHz range to perform low-frequency measurements. When using a vacuum-squeezed field in the MHz range, a 2 dB phase noise improvement beyond the SNL is achieved at a frequency of tens of kHz. Interestingly, the shot noise reduction

a)Electronic mail: zhangyong@nju.edu.cn
b)Electronic mail: jiaxj@sxu.edu.cn

of the interferometer does not vary with modulation depth in the current experimental configuration.

Figure 1 shows a schematic diagram of the squeezing-enhanced MZI. A coherent field $\hat{A}_0 = \hat{a}_0 e^{i\omega_0 t}$ at an optical carrier frequency of ω_0 is initially amplitude-modulated by an electro-optical modulator (EOM). This AM optical field can be written as

$$\hat{A} = \frac{\hat{a}_0}{2} e^{i\omega_0 t}\left[1 + e^{i(M\sin\Omega t+\phi)}\right] \approx \frac{\hat{a}_0}{2} e^{i\omega_0 t}\left[1 + e^{i\phi}\left(J_0 + J_1 e^{i\Omega t} - J_1 e^{-i\Omega t}\right)\right]. \quad (1)$$

Here, the modulation signal is $V = V_0 \sin\Omega t$, where Ω is the modulation frequency, $M = \pi V_0/V_\pi$ is the modulation depth, V_π is the half-wave voltage of the EOM, ϕ is the phase shift induced by the EOM, and $J_k = J_k(M)$ $(k = 0, 1)$ is the kth-order Bessel function.[34] In the experiments, the modulation depth $M < 1$, and the higher-order sidebands $(k \geq 2)$ are relatively small and can be neglected. In our scheme, Ω is set at 2.5 MHz to match the high-frequency squeezed state. The maximum modulation gain is obtained when the EOM is operating at $\phi = \pi/2$.

The modulated coherent state $\hat{A}$ and a squeezed vacuum state $\hat{B} = \hat{b}e^{i\omega_0 t}$ are then injected into the MZI from the two input ports. Using a linear operator method, we obtain $\hat{a}_0 = a_0 + \delta\hat{a}(t)$ and $\hat{b} = \delta\hat{b}(t)$, where $\delta\hat{a}(t)$ and $\delta\hat{b}(t)$ are the operator fluctuations. The mean values of $\delta\hat{a}(t)$ and $\delta\hat{b}(t)$ are zero. The linear operator of a modulated coherent mode with maximum modulation gain is

$$\hat{a} = \frac{1}{2}(a_0 + \delta\hat{a})\left[1 + i\left(J_0 + J_1 e^{i\Omega t} - J_1 e^{-i\Omega t}\right)\right]. \quad (2)$$

Using the matrix for a lossless 50/50 beam splitter, the balanced heterodyne detector's output signal is given by

$$\begin{aligned} n_{cd} &= \hat{c}^\dagger\hat{c} - \hat{d}^\dagger\hat{d} \\ &= \left(\hat{a}^\dagger\hat{a} - \hat{b}^\dagger\hat{b}\right)\cos\varphi + i\sin\varphi\left(\hat{b}^\dagger\hat{a}e^{-i\theta} - \hat{a}^\dagger\hat{b}e^{i\theta}\right) \\ &\approx \left(\frac{1+J_0^2}{4} - J_1\sin\Omega t + J_1^2\sin^2\Omega t\right)\left(a_0^2 + a_0\delta\hat{X}_a\right)\cos\varphi \\ &\quad + ia_0\left(J_1\sin\Omega t - \frac{1}{2}\right)\left(\delta\hat{b}e^{i\theta} - \delta\hat{b}^\dagger e^{-i\theta}\right)\sin\varphi \\ &\quad - \frac{1}{2}J_0 a_0\left(\delta\hat{b}e^{i\theta} + \delta\hat{b}^\dagger e^{-i\theta}\right)\sin\varphi, \end{aligned} \quad (3)$$

where $\hat{c}$ and $\hat{d}$ are the annihilation operators for the light beams after the beam splitter, θ is the relative phase between fields $\hat{a}$ and $\hat{b}$, and φ is the relative phase between the two MZI channels. The product terms of the fluctuations are omitted, given that $|\delta\hat{a}| \ll a_0$ and $|\delta\hat{b}| \ll b_0$. The output mode is demodulated using a local oscillator (LO) field of $V_{LO}(\cos\Omega t + \phi_{\mathrm{mod}})$. After passing through a low-pass filter, the generated signal is then given by

$$n_{cd} = -J_1(a_0^2 + a_0\delta\hat{X}_a)\cos\varphi + a_0 J_1\delta\hat{X}_b^{\theta+\pi/2}\sin\varphi, \quad (4)$$

with $\delta\hat{X}_b^\theta = \delta\hat{b}e^{i\theta} + \delta\hat{b}^\dagger e^{-i\theta}$. In the experiment, the phase φ is stabilized close to $(2m+1)\pi/2$ $(m = 0, 1, 2,\ldots)$. If we define $\varphi = (2m+1)\pi/2 + \varphi'$ with $\varphi' \ll 1$, then the output signal can be written as

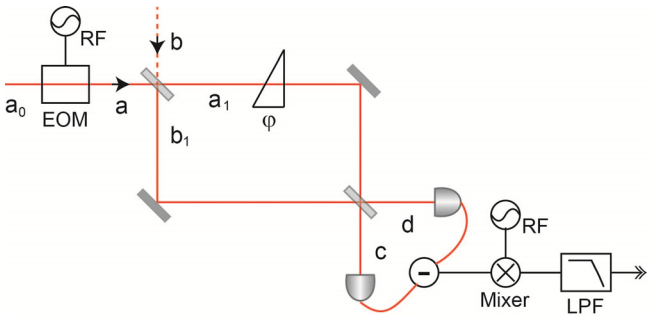

FIG. 1. Theoretical model of squeezing-enhanced MZI. Amplitude-modulated coherent light (a) and vacuum squeezed light (b) are used in our experimental setup. φ is the relative phase between the two arms of the interferometer. EOM: electro-optical modulator; LPF: low-pass filter.

$$n_{cd} \approx a_0^2 J_1\varphi' + a_0 J_1\delta\hat{X}_b^{\theta+\pi/2}. \quad (5)$$

In our experimental configuration, φ' is the parameter to be measured, and this parameter varies at a frequency of several tens of kHz. The phase error is given by

$$\Delta\varphi' = \frac{\Delta n_{cd}}{\partial\langle n_{cd}\rangle/\partial\varphi} = \frac{a_0 J_1\Delta\left(\delta X_b^{\theta+\pi/2}\right)}{a_0^2 J_1} = \frac{\Delta\left(\delta X_b^{\theta+\pi/2}\right)}{a_0}. \quad (6)$$

In the classical case with vacuum state $\hat{B}$, we have $\Delta(\delta X_b^{\theta+\pi/2}) = 1$ and $\Delta\varphi' = 1/\sqrt{N}$ (where $N = |a_0|^2$ is the average number of photons). If we use a phase-quadrature squeezed vacuum state at high frequency, we can then achieve $\Delta(\delta X_b^{\theta+\pi/2}) = e^{-r}$ with $\theta = 0$, where r is the squeezing factor. Clearly, the phase noise of the MZI is improved by a factor of e^{-r} in the low-frequency band. This quantum enhancement can also be achieved by inputting an amplitude-quadrature squeezed vacuum state with $\theta = \pi/2$. Interestingly, we can deduce from Eq. (6) that the modulation depth has no effect on the phase noise improvement when using this scheme.

Figure 2(a) shows the quantum source used in the experiments and Fig. 2(b) is a depiction of the experimental setup. The squeezed state of light is produced using a nondegenerate optical parametric amplifier (NOPA).[35] The NOPA cavity is a semi-monolithic optical resonator formed using an α-cut wedged type-II potassium titanyl phosphate (KTP) crystal and a concave mirror with radius of curvature of 50 mm. The NOPA is pumped using a continuous-wave Nd:YAP/LBO (Nd-doped $YAlO_3/LiB_3O_5$) laser that outputs both 1080 nm and 540 nm waves (CDPSSFG-VIB, Yu-Guang Co. Ltd.). The NOPA operates below the threshold in a deamplification mode, i.e., the phase difference between pump and injected beam is $(2n+1)\pi$ (where $n = 0, 1, 2,\ldots$). In our experiments, the NOPA pump power at 540 nm is approximately 75 mW and the signal intensity at 1080 nm is 10 mW. The output mode in the $-45°$ (or $+45°$) polarization direction from the NOPA is a vacuum squeezed state (or bright coherent squeezed state), which is a quadrature-phase squeezed state (or quadrature-amplitude squeezed state). After it passes through a half-wave plate and a polarizing

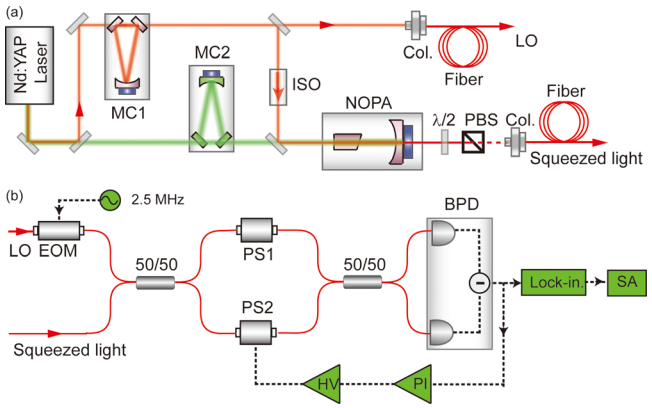

FIG. 2. Schematic diagram of squeezing-enhanced fiber MZI. (a) Continuous-wave laser with 1080 nm and 540 nm outputs used to produce squeezed light. (b) Squeezed light is coupled into the fiber MZI to measure the low-frequency phase signal. MC1: 1080 nm mode cleaner; MC2: 540 nm mode cleaner; ISO: isolator; NOPA: nondegenerate optical parametric amplifier; Col: fiber collimator; EOM: electro-optic modulator; 50/50: 50/50 fiber coupler; PSs: fiber phase shifters; BPD: balanced photodetector; Lock-in: lock-in amplifier; SA: spectrum analyzer; PI: PID servo; and HV amp: high-voltage amplifier.

beam splitter (PBS), the selected vacuum squeezed field is coupled into a polarization-maintaining fiber, which serves as the quantum source for the fiber MZI in our experiments. The fiber coupling efficiency is ~80%. Figure 3 shows the characteristics of the squeezed light that is coupled into the fiber using a balanced homodyne detector. In Fig. 3(a), trace (i) shows the SNL when measured with the squeezed light being blocked, while trace (ii) represents the quadrature noise in the vacuum squeezed state produced by linear sweeping of the local oscillator (LO) phase. The experimentally measured squeezing is 4 dB at 2.5 MHz, while the corresponding anti-squeezing is 8 dB. In the measurements, the escape efficiency is 97.6%, the detector quantum efficiency is 90%, and the interference efficiency is 99%. The photon detector dark noise is 20 dB below the vacuum noise. The broadband noise spectrum of the squeezing source is shown in Fig. 3(b), which represents reliable performance within a bandwidth of 100 kHz.

The fiber MZI in Fig. 2(b) is based on two 2×2 polarization-maintaining fiber couplers with 50/50 coupling ratios. Each MZI arm is 10 m long. Two fiber phase shifters (PS1 and PS2 in Fig. 2) driven by a piezoelectric transducer (PZT) are used to control the relative phase φ between the MZI arms. The half-wave voltages of both PS1 and PS2 are 11 V at 1080 nm. For enhanced precision, the optical loss in the fiber MZI must be suppressed as far as possible.[36–38] This loss can mainly be attributed to mode mismatch when the free-space squeezed field is coupled into the fiber. The fiber PS also introduces non-negligible losses. In the experiments, we use aspheric lenses with $f = 11$ mm to optimize fiber coupling. The total loss is controlled to within $40(\pm 1)\%$ in our system. Also, the optical losses of the two MZI arms are carefully balanced for the phase measurements. The input coherent field is amplitude-modulated at 2.5 MHz using an EOM (waveguide modulator, EOSpace). Its half-wave voltage is 3.5 V. At the other input port, the squeezed field is injected to produce the phase noise improvement beyond the SNL. At the MZI output ports, the interference signal is detected using a balanced photon-detector (BPD), which includes two InGaAs photodiodes (ETX500, JDS Uniphase Corporation). The low-frequency component (DC–10 kHz) from the BPD is amplified using a servo and is then fed back to PS2 to stabilize the relative phase φ of the MZI. The high-frequency component (>0.5 MHz) is sent to the lock-in amplifier for phase-sensitive detection at a modulation frequency of 2.5 MHz using a spectrum analyzer.

In the experiments, the LO field carries an amplitude modulation at 2.5 MHz for the phase measurements. The cut-off frequency of the low-pass filter contained in the lock-in amplifier is 300 kHz. At a modulation depth of 0.16, the shot noise is 25 dB above the dark noise at the same LO power shown in Fig. 2. The phase noise of the fiber MZI is measured by slowly sweeping the LO field phase with a linear ramp. Phase noise measurements are performed at several frequencies (from 30 kHz to 150 kHz with a step of 10 kHz), and show shot noise reduction in the fiber MZI (Fig. 4(a)). Figures 4(b), 4(c), and 4(d) show experimental results obtained at frequencies of 30, 80, and 150 kHz, respectively. When compared with the phase noise obtained without the squeezing state, as shown by the black curves in Figs. 4(b)–4(d), a 2 dB phase noise improvement is achieved, as indicated by the red curves. The measured escape efficiency, propagation efficiency (including fiber coupling efficiency at the MZI input ports), detector quantum efficiency, and interference efficiency are 97.6%, 60%, 90%, and 99%, respectively. From Eq. (6), the theoretical quantum improvement is calculated to be 2.4 dB, which agrees well with the experimental results.

Figure 5 shows the dependence of the phase noise reduction of the fiber interferometer on the EOM's amplitude

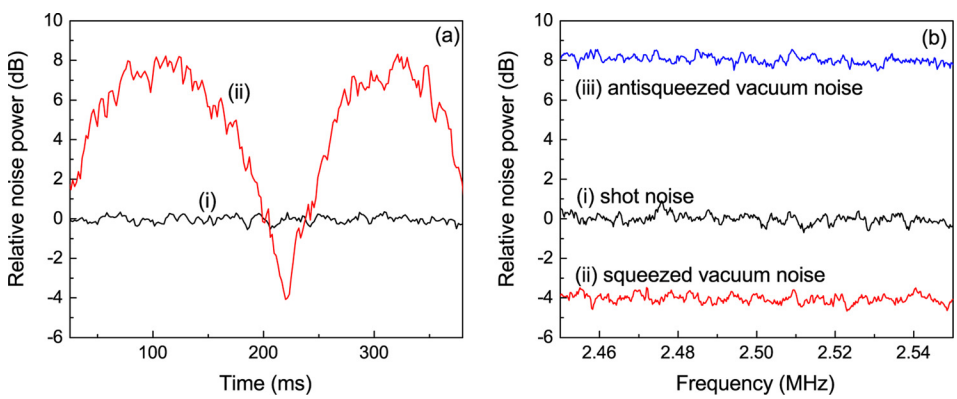

FIG. 3. (a) Noise power of squeezing source, measured at a sideband frequency of 2.5 MHz by linear sweeping of the LO phase before it enters the interferometer. Here, (i) is the shot noise limit; (ii) is the quadrature noise in the vacuum squeezed state. RBW = 3 kHz; VBW = 30 Hz; and sweep time = 700 ms. (b) Noise spectra of squeezing source within frequency band of 100 kHz.

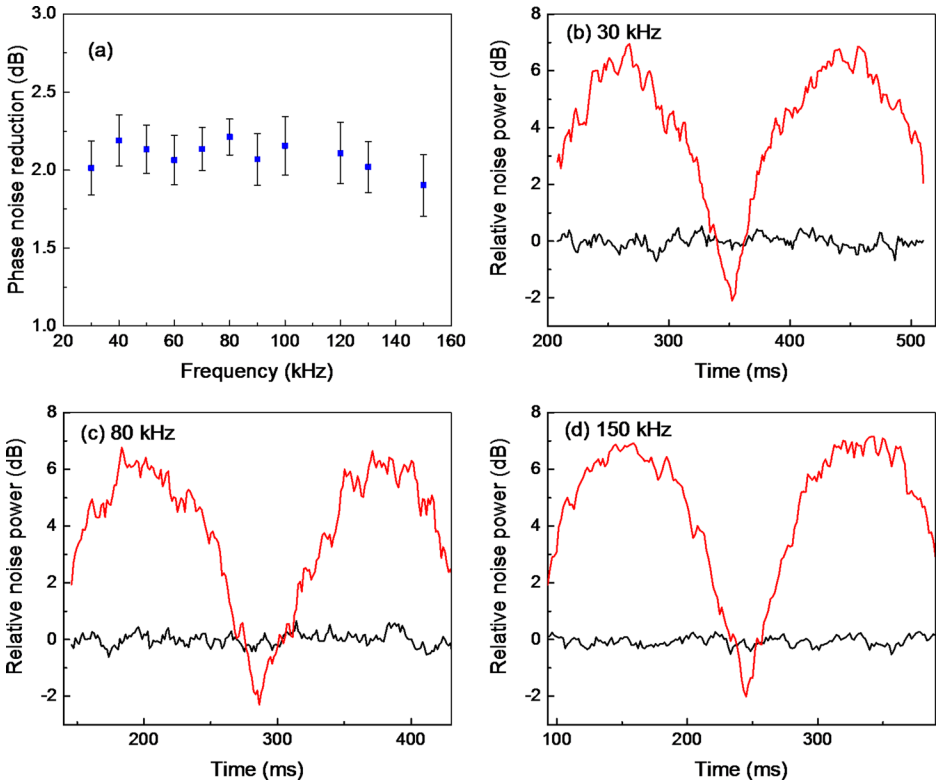

FIG. 4. (a) Measured phase noise of quantum-enhanced fiber interferometer for several frequencies (from 30 kHz to 150 kHz, in steps of 10 kHz). (b)–(d) The demodulated noise spectra of the interferometer output at 30 kHz, 80 kHz, and 150 kHz, respectively. The photodetector dark noise is 25 dB below the vacuum noise, which has been subtracted from the data. RBW = 3 kHz, VBW = 30 Hz, and sweep time = 700 ms.

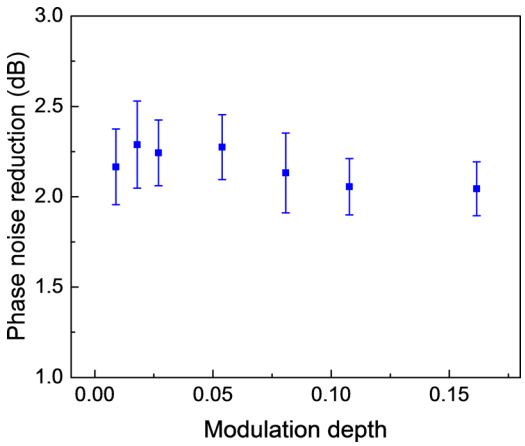

FIG. 5. Dependence of phase noise reduction on the modulation depth of EOM. The spectrum analyzer center frequency is set at 80 kHz.

modulation depth. In the theoretical model, the shot noise reduction defined using Eq. (6) indicates that it is not dependent on the modulation depth when using our scheme. Experimentally, we vary the modulation depth from 0.01 to 0.16 at a measurement frequency of 80 kHz while maintaining LO power at 4.15 mW. As shown in Fig. 5, the shot noise reduction of the fiber interferometer is maintained at approximately 2 dB while the modulation depth varies; this is consistent with theoretical predictions.

In conclusion, we have experimentally demonstrated a squeezing-enhanced fiber MZI for low-frequency phase measurements. By injecting an AM coherent field and performing balanced heterodyne detection, the high-frequency (MHz) squeezed state can be used to enhance low-frequency (kHz) phase noise measurements. A 2 dB quantum improvement beyond the SNL in an audio frequency was obtained experimentally. Also, the shot noise reduction under the proposed scheme is independent of modulation depth. The fiber MZI performance can be improved by further increasing the degree of squeezing at the input port and suppressing system losses. Our result broadens the potential range of applications when using fiber-based setups for quantum-enhanced sensing, particularly in the low-frequency range.

This work was supported by the National Basic Research Program of China (Grant No. 2016YFA0302500), the National Science Foundation of China (Grant Nos. 61605072, 91636106, 11322440, and 11654002), and the Fok Ying Tung Education Foundation.

[1]J. Aasi, J. Abadie, B. P. Abbott, R. Abbott, T. D. Abbott, M. R. Abernathy, C. Adams, T. Adams, P. Addesso, R. X. Adhikari *et al.*, Nat. Photonics **7**, 613 (2013).
[2]H. Yonezawa, D. Nakane, T. A. Wheatley, K. Iwasawa, S. Takeda, H. Arao, K. Ohki, K. Tsumura, D. W. Berry, T. C. Ralph *et al.*, Science **337**, 1514 (2012).
[3]V. Giovannetti, S. Lloyd, and L. Maccone, Science **306**, 1330 (2004).
[4]S. Steinlechner, J. Bauchrowitz, M. Meinders, H. Muller-Ebhardt, K. Danzmann, and R. Schnabel, Nat. Photonics **7**, 626 (2013).
[5]K. Goda, O. Miyakawa, E. E. Mikhailov, S. Saraf, R. Adhikari, K. McKenzie, R. Ward, S. Vass, A. J. Weinstein, and N. Mavalvala, Nat. Phys. **4**, 472 (2008).
[6]J. Xin, H. L. Wang, and J. T. Jing, Appl. Phys. Lett. **109**, 051107 (2016).
[7]B. P. Abbott, R. Abbott, T. D. Abbott, M. R. Abernathy, F. Acernese, K. Ackley, C. Adams, T. Adams, P. Addesso, R. X. Adhikari *et al.*, Phys. Rev. Lett. **116**, 061102 (2016).
[8]C. K. Kirkendall and A. Dandridge, J. Phys. D: Appl. Phys. **37**, R197 (2004).
[9]W. H. Glenn, IEEE J. Quantum Electron. **25**, 1218 (1989).
[10]J. H. Chow, D. E. McClelland, M. B. Gray, and I. C. M. Littler, Opt. Lett. **30**, 1923 (2005).
[11]X. Wang, S. Y. Chen, Z. G. Du, X. Y. Wang, C. H. Shi, and J. P. Chen, IEEE Sens. J. **8**, 1173 (2008).
[12]G. Gagliardi, M. Salza, S. Avino, P. Ferraro, and P. De Natale, Science **330**, 1081 (2010).

[13]T. G. McRae, S. Ngo, D. A. Shaddock, M. T. L. Hsu, and M. B. Gray, Opt. Lett. **38**, 278 (2013).
[14]C. M. Caves, Phys. Rev. D **23**, 1693 (1981).
[15]M. Xiao, L. A. Wu, and H. J. Kimble, Phys. Rev. Lett. **59**, 278 (1987).
[16]P. Grangier, R. E. Slusher, B. Yurke, and A. Laporta, Phys. Rev. Lett. **59**, 2153 (1987).
[17]L. S. Collaboration, Nat. Phys. **7**, 962 (2011).
[18]T. Eberle, S. Steinlechner, J. Bauchrowitz, V. Handchen, H. Vahlbruch, M. Mehmet, H. Muller-Ebhardt, and R. Schnabel, Phys. Rev. Lett. **104**, 251102 (2010).
[19]L. A. Wu, M. Xiao, and H. J. Kimble, J. Opt. Soc. Am. B **4**, 1465 (1987).
[20]R. E. Slusher, L. W. Hollberg, B. Yurke, J. C. Mertz, and J. F. Valley, Phys. Rev. Lett. **55**, 2409 (1985).
[21]Y. Zhang, H. Wang, X. Y. Li, J. T. Jing, C. D. Xie, and K. C. Peng, Phys. Rev. A **62**, 023813 (2000).
[22]M. Mehmet, S. Ast, T. Eberle, S. Steinlechner, H. Vahlbruch, and R. Schnabel, Opt. Express **19**, 25763 (2011).
[23]K. McKenzie, N. Grosse, W. P. Bowen, S. E. Whitcomb, M. B. Gray, D. E. McClelland, and P. K. Lam, Phys. Rev. Lett. **93**, 161105 (2004).
[24]K. McKenzie, D. A. Shaddock, D. E. McClelland, B. C. Buchler, and P. K. Lam, Phys. Rev. Lett. **88**, 231102 (2002).
[25]H. Vahlbruch, S. Chelkowski, B. Hage, A. Franzen, K. Danzmann, and R. Schnabel, Phys. Rev. Lett. **97**, 011101 (2006).
[26]A. Khalaidovski, H. Vahlbruch, N. Lastzka, C. Graf, K. Danzmann, H. Grote, and R. Schnabel, Classical Quantum Gravity **29**, 075001 (2012).
[27]H. Grote, K. Danzmann, K. L. Dooley, R. Schnabel, J. Slutsky, and H. Vahlbruch, Phys. Rev. Lett. **110**, 181101 (2013).
[28]C. J. Liu, J. T. Jing, Z. F. Zhou, R. C. Pooser, F. Hudelist, L. Zhou, and W. P. Zhang, Opt. Lett. **36**, 2979 (2011).
[29]M. S. Stefszky, C. M. Mow-Lowry, S. S. Y. Chua, D. A. Shaddock, B. C. Buchler, H. Vahlbruch, A. Khalaidovski, R. Schnabel, P. K. Lam, and D. E. McClelland, Classical Quantum Gravity **29**, 145015 (2012).
[30]J. Geabanacloche and G. Leuchs, J. Mod. Opt. **34**, 793 (1987).
[31]B. Yurke, P. Grangier, and R. E. Slusher, J. Opt. Soc. Am. B **4**, 1677 (1987).
[32]Z. H. Zhai and J. R. Gao, Opt. Express **20**, 18173 (2012).
[33]R. G. Yang, J. Zhang, Z. H. Zhai, S. Q. Zhai, K. Liu, and J. R. Gao, Opt. Express **23**, 21323 (2015).
[34]H. Shen, L. Li, J. Bi, J. Wang, and L. Chen, Phys. Rev. A **92**, 063809 (2015).
[35]Y. Y. Zhou, X. J. Jia, F. Li, C. D. Xie, and K. C. Peng, Opt. Express **23**, 4952 (2015).
[36]M. Mehmet, T. Eberle, S. Steinlechner, H. Vahlbruch, and R. Schnabel, Opt. Lett. **35**, 1665 (2010).
[37]V. Giovannetti, S. Lloyd, and L. Maccone, Nat. Photonics **5**, 222 (2011).
[38]J. Joo, W. J. Munro, and T. P. Spiller, Phys. Rev. Lett. **107**, 083601 (2011).